



CrossMark
click for updates

Cite this: *Chem. Sci.*, 2017, 8, 1454

Mechanistic study of the rhodium-catalyzed carboxylation of simple aromatic compounds with carbon dioxide†

Takuya Suga, Takanobu Saitou, Jun Takaya and Nobuharu Iwasawa*

A detailed mechanism of the Rh(I)-catalyzed carboxylation of simple aromatic compounds *via* C–H bond activation was investigated. Kinetic studies with model compounds of the postulated key intermediates revealed that 14-electron complexes, RhMe(dcype) and RhPh(dcype), participated in the C–H bond activation step and the carboxylation step, respectively. Interestingly, the undesired carboxylation of RhMe(dcype) to give acetic acid was found to be much faster than the desired C–H bond activation reaction under stoichiometric conditions, however, the C–H bond activation reaction could occur under catalytic conditions. Careful controlled experiments revealed that C–H bond activation using RhMe(dcype) became competitive with its direct carboxylation under the condition that the concentration of CO₂ in the liquid phase was rather low. This factor could be controlled to some extent by mechanical factors such as the stirring rate and the shape of the reaction vessel. The resting state of the rhodium species under catalytic conditions was found to be [RhCl(dcype)]₂, and the proposed intermediates such as RhMe(dcype) and Rh(OBz)(dcype) were readily converted to the most stable state, [RhCl(dcype)]₂, *via* transmetalation with [Al]–Cl species, thus preventing the decomposition of the active catalytic species.

Received 27th August 2016

Accepted 11th October 2016

DOI: 10.1039/c6sc03838g

www.rsc.org/chemicalscience

Introduction

Catalytic direct carboxylation of simple hydrocarbons with carbon dioxide (CO₂) is a formidable challenge in organic chemistry.¹ Recently, we reported Rh(I)-catalyzed carboxylation of simple aromatic compounds such as benzene and toluene using a combination of [RhCl(dcype)]₂ **1** (dcype: 1,2-bis(dicyclohexylphosphino)ethane) and AlMe_{1.5}(OEt)_{1.5} as a stoichiometric methylating agent (Scheme 1).^{2–4} The most attractive feature of this reaction is its wide generality. Not only electron poor/rich arenes, but also heteroareamics such as benzofuran and indole were carboxylated successfully. Furthermore, ferrocene showed remarkable reactivity in this reaction.

The proposed reaction mechanism is shown in Scheme 2. The reaction starts with the generation of a 14-electron methylrhodium(I) complex **A** through transmetalation of [RhCl(dcype)]₂ **1** with AlMe_{1.5}(OEt)_{1.5}, followed by oxidative addition of an sp² C–H bond of benzene to **A**, giving phenyl(hydrido)(methyl)rhodium(III) intermediate **B**. Reductive elimination of methane from **B** affords a reactive 14-electron phenylrhodium(I) complex **C**.⁵ Nucleophilic addition of **C** to CO₂ gives a rhodium(I) benzoate complex

D,⁶ which is converted to methylrhodium(I) **A** through transmetalation with AlMe_{1.5}(OEt)_{1.5}.

The key to our success consists of three main factors. The first is the choice of methylrhodium(I) as the C–H activation species. It was reported as a stoichiometric reaction by Andersen's and Field's groups that heating or photoirradiating methylrhodium(I) species in benzene afforded the corresponding phenylrhodium(I) species.⁵ It was expected that by using methylrhodium(I) species, the irreversible dissociation of methane from intermediate **B** would give the desired arylrhodium(I) species efficiently. The second is the reactivity of RhMe(dcype) **A**. For the success of the

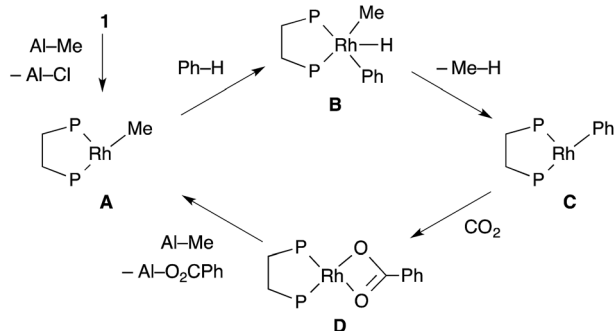


Scheme 1 Rh-Catalyzed C–H bond carboxylation.

Department of Chemistry, Tokyo Institute of Technology, O-okayama, Meguro-ku, Tokyo 152-8551, Japan. E-mail: niwasawa@chem.titech.ac.jp

† Electronic supplementary information (ESI) available: Experimental details and crystallographic data in cif format. CCDC 1017905. For ESI and crystallographic data in CIF or other electronic formats see DOI: 10.1039/c6sc03838g





Scheme 2 Postulated reaction mechanism.

preparation of benzoic acid, direct carboxylation of **A** to produce acetic acid should be slower than the C–H bond activation of benzene by **A**. If the direct carboxylation was much faster than the C–H bond activation, the reaction would produce acetic acid only. The third one is the choice of the methylating agent to regenerate **A**. Methylaluminum was selected because it is widely known to be reactive for transmetalation, but it does not directly react with CO₂ under appropriate conditions. Other reagents such as MeMgBr are unsuitable for this reason.

Apart from its synthetic utility, a noteworthy feature of this reaction is the realization of C–H bond activation followed by nucleophilic addition using the combination of a low-valence transition metal catalyst and a stoichiometric alkylating agent. Such C–H bond functionalization strategies are quite limited and most of the reported C–H activation-nucleophilic addition reactions utilize high-valence transition metal complexes such as Rh(III) for C–H bond activation.⁷ In 2010, we reported the first example of such reaction, that is, rhodium-catalyzed direct carboxylation of 2-phenylpyridines.⁸ In 2012, Yoshikai reported a catalytic C–H bond activation of 2-phenylpyridine derivatives using the combination of a cobalt catalyst and a stoichiometric organomagnesium reagent, followed by nucleophilic addition to *N*-arylimines.⁹ Very recently, Wang reported that the use of a manganese catalyst with a stoichiometric amount of dimethylzinc was effective for the coupling of 2-phenylpyridines with aldehydes and nitriles.^{10,11} This kind of catalytic nucleophilic addition is still limited, but would become a powerful methodology in C–H bond functionalization reactions.

As described above, several reactions have recently been reported for this type of C–H activation-nucleophilic addition reactions, however, there has been almost no detailed study on the mechanism of such reactions, probably because of the difficulty in capturing highly reactive alkyl or aryl transition metal intermediates. For example, confirmation of the intermediacy of the 14-electron complexes in the C–H activation and carboxylation steps is not necessarily easy in our reaction because of their instability. As already described, stoichiometric reactivity of relevant methylrhodium(I) species to C–H bond activation has been known for more than three decades, but its detailed mechanistic study has not been carried out.⁵ Concerning the carboxylation step, there are several reports for stoichiometric carboxylation reactions of arylrhodium(I) complexes,⁶ however, their mechanisms have been proposed

only by theoretical studies.¹² Furthermore, transmetalation behaviors and resting states are also left unclarified. In this paper, we report a detailed analysis of the mechanism of this rhodium-catalyzed C–H carboxylation reaction based on kinetic studies using several model compounds, the examination of various reaction conditions including the shape of the reaction vessels and the stirring rate, analysis of the reaction mixture, and some controlled experiments.

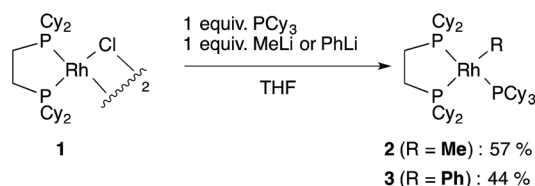
Results and discussion

1. Preparation and reactivity of tetracoordinated 16-electron rhodium species

To support the proposed reaction mechanism shown in Scheme 2, we initially tried to prepare each intermediate in the proposed catalytic cycle. In particular, 14-electron complexes RhMe(dcyPe) **A** and RhPh(dcyPe) **C** were the most attractive because they were thought to be true intermediates in the most important C–H bond activation and carboxylation steps.

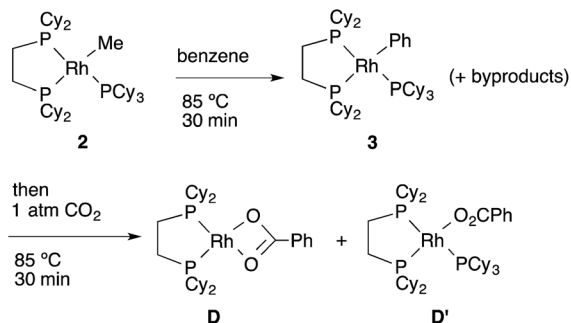
Tricoordinated 14-electron alkyrhodium complexes are known to be so unstable that, up to now, they had not been isolated except for few specific examples.¹³ Indeed, we initially attempted to prepare them by treating [RhCl(dcyPe)]₂ **1** with several methylating agents such as methyl lithium, methylmagnesium bromide and trimethylaluminum, however, all of our efforts turned out to be fruitless. Therefore, we decided to prepare the tetracoordinated 16-electron complexes RhMe(PCy₃)(dcyPe) **2** and RhPh(PCy₃)(dcyPe) **3** as appropriate precursors of the 14-electron complexes (Scheme 3).¹⁴ **2** and **3** were prepared in good yields through the treatment of [RhCl(dcyPe)]₂ with MeLi and PhLi, respectively in the presence of a stoichiometric amount of PCy₃.¹⁵ Their structures were determined using ¹H and ³¹P NMR. **3** was also characterized using single crystal X-ray structure analysis (see ESI†).

Next, the reactivity of these complexes for the C–H bond activation and carboxylation reactions was examined. To our delight, RhMe(PCy₃)(dcyPe) **2** was found to react with benzene to give RhPh(PCy₃)(dcyPe) **3** under argon at 85 °C with perfect conversion although partial decomposition was also observed (Scheme 4). Moreover, further exposure of this solution to 1 atm CO₂ at 85 °C gave a mixture of the carboxylated products Rh(O₂CPh)(dcyPe) **D** and Rh(O₂CPh)(PCy₃)(dcyPe) **D'** (**D** : **D'** = 1 : 2 at room temperature). No intermediates were observed in these two reactions. The rhodium benzoates were characterized by comparing their ³¹P NMR spectra with those of authentic samples of **D** and **D'** (see ESI† for their preparative methods).



Scheme 3 Preparation of model complexes.





Scheme 4 Reactions of model complexes.

2. Mechanistic study on C–H bond activation by methylrhodium(i) species

With the suitable model complexes in hand, we carried out a kinetic study of the C–H bond activation step by monitoring the reaction with ^1H NMR (Fig. 1). The rate of the C–H bond activation reaction of $\text{RhMe}(\text{PCy}_3)_2(\text{dcype})$ **2** with benzene- d_0 as a solvent was measured in the presence of various concentrations of PCy_3 . Fortunately, the addition of PCy_3 completely suppressed decomposition of the complex, and the desired transformation proceeded quantitatively according to the ^{31}P NMR spectra (see ESI†).¹⁶ The reaction was found to be first

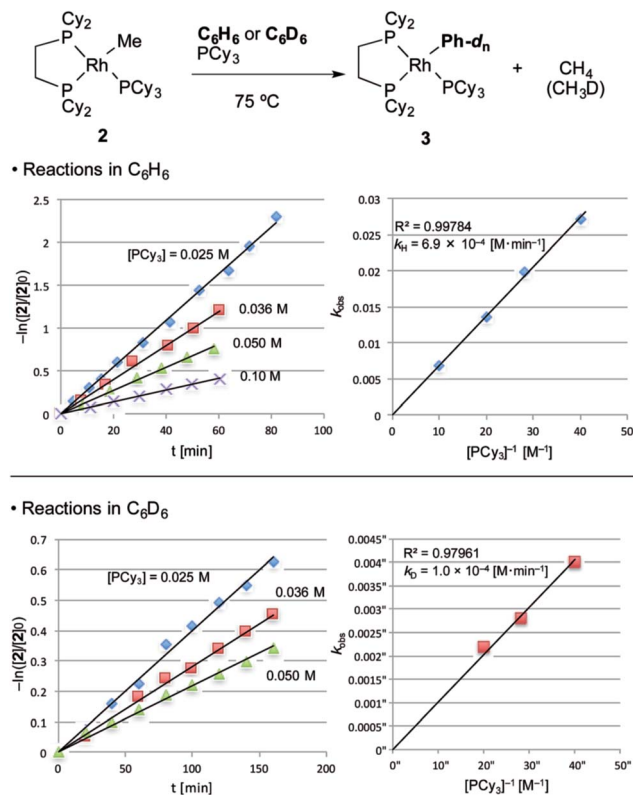


Fig. 1 Kinetics of C–H bond activation. Conditions: 0.005 mmol **2**, 0.50 mL benzene in an NMR tube under argon. The reaction was analyzed using ^1H NMR. Consumption of **2** was traced with the decay of the signal at $\delta = 0.4$ (RhCH_3). No other products were observed using ^{31}P NMR after the reaction.

order to $\text{RhMe}(\text{PCy}_3)_2(\text{dcype})$ **2** and inverse first order to PCy_3 (eqn (1)).

$$-\ln([2]/[2]_0) = k_{\text{H(D)}}[\text{PCy}_3]^{-1}t \quad (1)$$

$$k_{\text{H}} = 6.9 \times 10^{-4} [\text{M min}^{-1}]$$

$$k_{\text{D}} = 1.0 \times 10^{-4} [\text{M min}^{-1}]$$

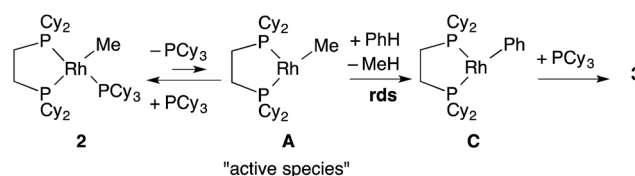
$$k_{\text{H}}/k_{\text{D}} = 6.9$$

The value of $-\ln([2]/[2]_0)$ was completely proportional to the reaction time even after 90% conversion, and was inversely proportional to $[\text{PCy}_3]$ with the rate constant $k_{\text{H}} = 6.9 \times 10^{-4} [\text{M min}^{-1}]$ at 75°C . According to the steady state approximation, this reaction includes dissociation of PCy_3 before the rate-determining step. In addition, the reaction in benzene- d_6 was apparently slower ($k_{\text{D}} = 1.0 \times 10^{-4} [\text{M min}^{-1}]$) than in benzene- d_0 and the KIE value ($k_{\text{H}}/k_{\text{D}}$) was estimated to be 6.9. This large KIE value strongly suggests that the C–H bond activation step is rate-determining in this stoichiometric reaction.

With these results, it was concluded that tricoordinated $\text{RhMe}(\text{dcype})$ **A** is the true intermediate of the C–H bond activation step (Scheme 5). ^1H NMR analysis also indicated the formation of CH_4 in benzene- d_0 , and CH_3D in benzene- d_6 . The detailed process of C–H bond activation remains unclear through our study, but the oxidative addition–reductive elimination process should be the most plausible. For instance, Sakakura reported that photo-induced reaction of $\text{Rh}^{\text{III}}(\text{H})(\text{Cl})(\text{Ph})(\text{PMe}_3)_3$ in benzene generated $\text{Rh}^{\text{III}}(\text{H})(\text{Cl})(\text{Ph})(\text{PMe}_3)_3$.^{17,18}

The formation of methane was also confirmed using GC analysis of the reaction mixture under catalytic conditions (Fig. 2). After the catalytic carboxylation of benzene was carried out under optimized conditions using $[\text{RhCl}(\text{dcype})]_2$ **1** and $\text{AlMe}_{1.5}(\text{OEt})_{1.5}$, the gas phase of the resulting mixture was directly injected into the GC. While no methane formation was observed in the absence of $[\text{RhCl}(\text{dcype})]_2$ **1**, it was detected under catalytic conditions.

We also carried out several KIE studies under catalytic conditions to determine the turnover-limiting step. It should be noted that an accurate kinetic study of this reaction is difficult under our conditions because of the CO_2 concentration problem (noted in the later section) and complex disproportionation of the methylaluminum reagent. Therefore, the results described below may not be very precise but are sufficient for general discussion.



Scheme 5 Plausible pathway of the C–H bond activation step.



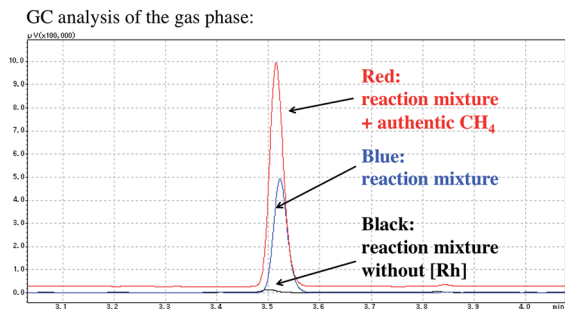


Fig. 2 Methane observation using GC analysis. The reaction was carried out in benzene at 85 °C. Detailed reaction conditions were the same as shown in Scheme 1.

The KIEs were measured using two procedures (Scheme 6). In procedure 1, the reaction was performed using a 1 : 1 mixture of benzene- d_0 and benzene- d_6 . In procedure 2, the reactions with benzene- d_0 and benzene- d_6 were carried out in separate vessels, and the resulting mixtures were combined after quenching the reaction with aqueous 1 M HCl. Both reactions were performed at 85 °C for 1 h. The ratio of benzoic acid- d_0 and benzoic acid- d_5 was estimated using ^1H NMR after esterification of the benzoic acids with benzyl bromide. As a result, $[5-d_0]/[5-d_5] = 5.5$ (procedure 1) and $[5-d_0]/[5-d_5] = 4.0$ (procedure 2) were obtained. These large KIE values indicate that the C–H bond activation step is also the turnover-limiting step under catalytic conditions.

3. Mechanistic study of the carboxylation step

Next, a kinetic study of the carboxylation reaction of $\text{RhPh}(\text{PCy}_3)(\text{dcype})$ **3** was carried out under CO_2 (1 atm at 22–23 °C) in the presence of PCy_3 in toluene- d_8 (Fig. 3).¹⁹ The value of $-\ln([3]/[3]_0)$ was proportional to the reaction time and was almost inversely proportional to $[\text{PCy}_3]$ with the rate

constant $k_{\text{Ph1}} = 2.5 \times 10^{-3} [\text{M min}^{-1}]$ at 35 °C (eqn (2)), suggesting that the carboxylation step is much faster than the C–H activation step, which coincided with the results of the KIE studies.

$$-\ln([3]/[3]_0) = (k_{\text{Ph1}}[\text{PCy}_3]^{-1} + k_{\text{Ph2}})t \quad (2)$$

$$k_{\text{Ph1}} = 2.5 \times 10^{-3} [\text{M min}^{-1}]$$

$$k_{\text{Ph2}} = 8.0 \times 10^{-3} [\text{min}^{-1}]$$

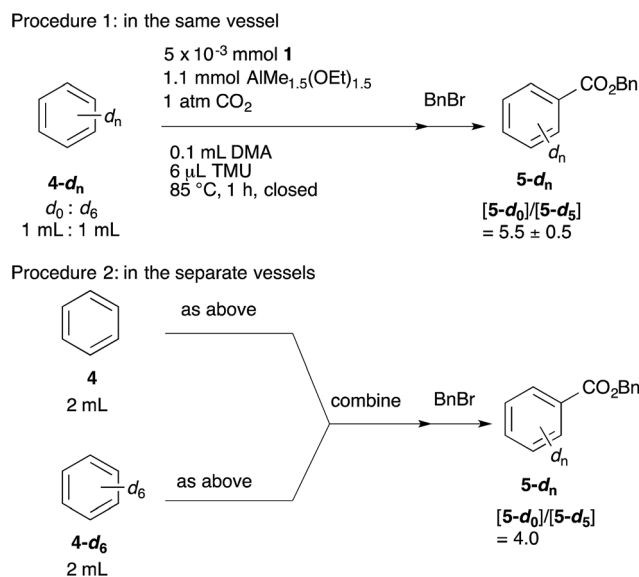
Dissociation of PCy_3 was also clearly involved in the carboxylation step. The small intercept term $k_{\text{Ph2}} = 8.0 \times 10^{-3} [\text{min}^{-1}]$ left the possibility of a minor pathway (*e.g.* the reaction without dissociation of PCy_3), but it was trivial at lower concentrations of PCy_3 . Therefore, it is concluded that the carboxylation step mainly proceeded *via* 14-electron complex $\text{RhPh}(\text{dcype})\text{C}$ in a similar manner to the C–H bond activation step (Scheme 7).

The carboxylation reaction of $\text{RhMe}(\text{PCy}_3)(\text{dcype})$ **2** was also carried out in toluene- d_8 at 35 °C (Fig. 4).²⁰ **2** showed a somewhat lower reactivity of carboxylation compared to $\text{RhPh}(\text{PCy}_3)(\text{dcype})$ **3** (eqn (3), $k_{\text{Me1}} = 1.0 \times 10^{-3} [\text{M min}^{-1}]$ vs. $k_{\text{Ph1}} = 2.5 \times 10^{-3} [\text{M min}^{-1}]$).

$$-\ln([2]/[2]_0) = k_{\text{Me1}}[\text{PCy}_3]^{-1}t \quad (3)$$

$$k_{\text{Me1}} = 1.0 \times 10^{-3} [\text{M min}^{-1}]$$

The equation was similar to that of $\text{RhPh}(\text{PCy}_3)(\text{dcype})$ **3** except for complete disappearance of the intercept term



Scheme 6 KIE study under catalytic conditions.

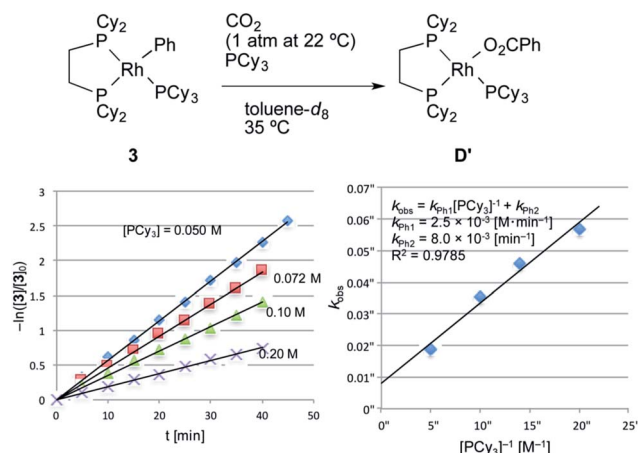
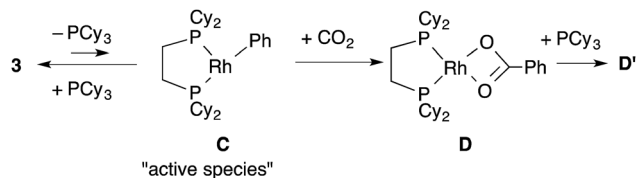


Fig. 3 Kinetics of the carboxylation of **3**. Conditions: 0.005 mmol **3**, 0.50 mL toluene- d_8 in an NMR tube (ca. 4 mL vol.) under 1 atm CO_2 . The solution was saturated with CO_2 at 22–23 °C beforehand (see ESI†). Consumption of **3** was traced with the decay of the signal at δ 7.9 ppm (Ph). No other products were observed using ^{31}P NMR after the reaction.





Scheme 7 Plausible pathway of the carboxylation step.

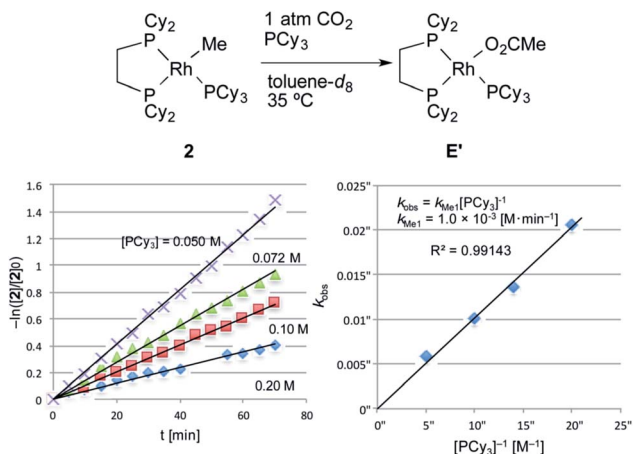
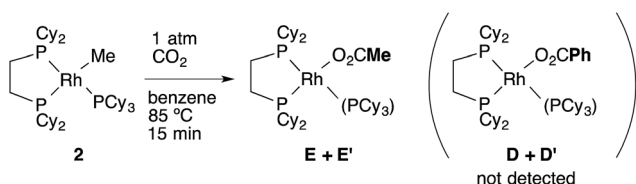


Fig. 4 Kinetics of the carboxylation of **2**. Conditions: 0.005 mmol **2**, 0.50 mL toluene- d_8 in an NMR tube (ca. 4 mL vol.) under 1 atm CO_2 . The solution was saturated with CO_2 at 22–23 °C beforehand (see ESI†). Consumption of **2** was traced with the decay of the signal at δ 0.4 ppm (CH_3).

($k_{\text{Me}2} = 0$), suggesting the intermediacy of $\text{RhMe}(\text{dcype})$ **A** as a reactive species. ^1H and ^{31}P NMR indicated that there was no formation of the C–H activation product $\text{Rh}(\text{tol})(\text{PCy}_3)(\text{dcype})$ or corresponding benzoates throughout the reaction. In addition, the stoichiometric reaction of $\text{RhMe}(\text{PCy}_3)(\text{dcype})$ **2** under 1 atm CO_2 in benzene at 85 °C did not give benzoates at all, but gave only acetates $\text{Rh}(\text{OAc})(\text{dcype})$ **E** and $\text{Rh}(\text{OAc})(\text{PCy}_3)(\text{dcype})$ **E'** (Scheme 8). These results imply that the carboxylation of $\text{RhMe}(\text{dcype})$ **A** with CO_2 proceeded much faster than the C–H activation of **A** with benzene under 1 atm CO_2 . In other words, predominant formation of acetic acid should associate with the formation of benzoic acid.

Based on the above considerations, the TON of acetic acid (AcOH) was estimated using GC analysis under catalytic conditions. According to the standard catalytic procedure, the reaction was carried out in a 40 cm^3 test tube for 6 h at 85 °C with the tube kept closed. As we expected, it was found that in

Scheme 8 Stoichiometric carboxylation of **2** at 85 °C.

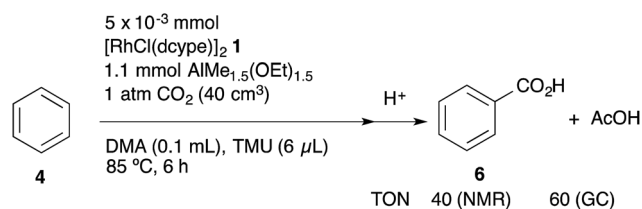
addition to ca. 0.40 mmol (TON = 40) of benzoic acid, ca. 0.6 mmol (TON = ca. 60) of acetic acid was produced as judged using GC analysis (Scheme 9). However, the ratio of $\text{BzOH} : \text{AcOH} = 2 : 3$ was still inconsistent with the result of the stoichiometric study. To obtain more information on the competitive formation of benzoic acid and acetic acid, we decided to carry out a more detailed analysis of the reactions to clarify the difference of these stoichiometric and catalytic reactions.

All the reactions so far have been carried out using 40 cm^3 test tube (ca. 2 mmol of CO_2 should be inside) in a closed system for the catalytic reaction, and ca. 1 mmol of CO_2 was consumed to produce benzoic acid and acetic acid as shown in Scheme 9. As the amount of CO_2 in the reaction mixture was thought to be influential on the ratio of carboxylic acids under catalytic conditions, the reaction was examined using several vessels with different shapes and volumes.

The effect of the reaction vessel was examined by changing the total volume and/or the shape of the reaction vessel (Table 1).²¹ The reaction time was set to 1 h to reduce the effects of catalyst decomposition and reagent consumption. The stirring rate was kept at ca. 800 rpm. The reaction vessels were; a 40 cm^3 test tube ($\phi = 2$ cm, vessel 1) with a closed system (entry 1), a 40 cm^3 test tube (vessel 1) with a 2000 cm^3 balloon filled with CO_2 to disregard the decrease of CO_2 in a whole vessel (entry 2), a 40 cm^3 round-bottom flask (vessel 2) with a 2000 cm^3 balloon (entry 3) and a 160 cm^3 round-bottom flask (vessel 3) with a closed system (entry 4). In entry 4, the content of CO_2 should also be sufficient (ca. 7 mmol).

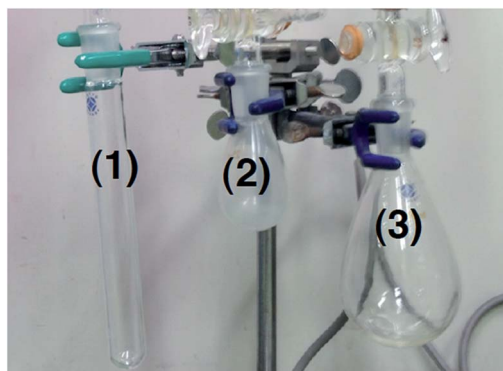
It was found that the volume of the vessel was not so influential on the ratio of benzoic acid and acetic acid, but the shape of the vessel caused a dramatic difference. The value of $[\text{BzOH}]/[\text{AcOH}]$ in vessel 1 was 0.12 without a balloon and 0.14 with a balloon (entry 1 vs. 2). This indicated that the total content of CO_2 was not responsible for the selectivity during the initial 1 h of reaction time.²² In sharp contrast, the use of vessel 2 decreased $[\text{BzOH}]/[\text{AcOH}]$ to 0.03 (entry 2 vs. 3). The formation of acetic acid was predominant when vessel 3 was employed (entry 4, $[\text{BzOH}]/[\text{AcOH}] = 0.01$) as observed in the reaction of $\text{RhMe}(\text{PCy}_3)(\text{dcype})$ **2** under CO_2 in benzene (Scheme 8).

This large effect of the shape of the vessel would be due to the dissolution rate of CO_2 into solution, which was elucidated using *in situ*-IR analysis at room temperature (Fig. 5).²³ CO_2 dissolution occurred more rapidly in a 40 cm^3 round-bottom flask than in a 40 cm^3 test tube even though they have almost the same total volume. For instance, the CO_2 concentration reached saturation within 200 seconds in the round-bottom



Scheme 9 Confirmation of acetic acid formation.



Table 1 Effect of the CO₂ content and shape of the vessel^a

| Entry | Conditions | Total volume (cm ³) | TON | | |
|-------|--------------------|---------------------------------|--------|--------|---------------|
| | | | [BzOH] | [AcOH] | [BzOH]/[AcOH] |
| 1 | Vessel 1 | 40 | 7.9 | 68 | 0.12 |
| 2 | Vessel 1 + balloon | 40 + 2000 | 5.7 | 42 | 0.14 |
| 3 | Vessel 2 + balloon | 40 + 2000 | 2.5 | 84 | 0.03 |
| 4 | Vessel 3 | 160 | 1.3 | 147 | 0.01 |

^a Vessel 1: 40 cm³ test tube ($\phi = 2$ cm), vessel 2: 40 cm³ round-bottom flask, vessel 3: 160 cm³ round-bottom flask. Conditions are shown in Scheme 9, except the reaction time was shortened to 1 h. Stirring rates were approx. 800 rpm.

flask. On the other hand, it took almost 1000 seconds in the test tube. Although the results shown here were obtained without stirring, the rate of dissolution of CO₂ certainly depends on the surface area of the solution, which influenced the ratio of BzOH and AcOH. For the same reason, the stirring rate was also found to be responsible (Table 2). Slower stirring gave an improved ratio of [BzOH]/[AcOH], although the total TON decreased. For example, [BzOH]/[AcOH] was 0.25 and the total TON was 41 at 100 rpm, while [BzOH]/[AcOH] was 0.07 and the total TON was 99 at 1000 rpm.

From these results, it was concluded that this reaction strongly depends on CO₂ concentration in the liquid phase, which was mainly determined by the dissolution rate of CO₂. In other words, the liquid phase is not saturated with CO₂ owing to its fast consumption by carboxylation reactions under catalytic

conditions. In the presence of sufficient CO₂, intermediate RhMe(dcype) A mostly reacts with CO₂ to give acetic acid before it reacts with benzene to give RhPh(dcype) C, as observed in entry 4 in Table 1 and entry 3 in Table 2, and this agrees with the result of the stoichiometric reaction of RhMe(PCy₃)(dcype) 2 in CO₂-saturated benzene. However, the true concentration of CO₂ should be rather low under catalytic conditions particularly with slower stirring and a liquid phase with a smaller surface area. Carboxylation and C–H bond activation of benzene by RhMe(dcype) A becomes competitive under such conditions, and both benzoic acid and acetic acid were obtained catalytically in contrast to the stoichiometric reaction of RhMe(PCy₃)(dcype) 2.

In summary, we proved that 14-electron tricoordinated RhPh(dcype) C is a plausible intermediate in the carboxylation step. RhMe(dcype) A also reacted with CO₂ in a similar way to give acetic acid catalytically. This undesired pathway was predominant over the desired C–H bond activation reaction under 1 atm CO₂. Nevertheless, C–H bond activation of benzene

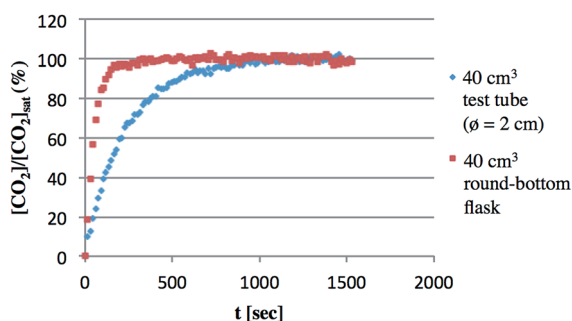


Fig. 5 Dissolution of CO₂ in toluene. Dissolution of CO₂ was traced using *in situ*-IR spectrometry (2350 cm⁻¹) in 2 cm³ toluene at room temperature. The mixtures were stood without stirring during measurement.

Table 2 Effect of stirring rate^a

| Entry | Rate [rpm] | TON | | |
|-------|------------|--------|--------|---------------|
| | | [BzOH] | [AcOH] | [BzOH]/[AcOH] |
| 1 | 100 | 8.3 | 33 | 0.25 |
| 2 | 800 | 7.9 | 68 | 0.12 |
| 3 | 1000 | 6.2 | 93 | 0.07 |

^a Reactions were carried out in 40 cm³ test tubes (closed system). Conditions were the same as noted in Table 1.



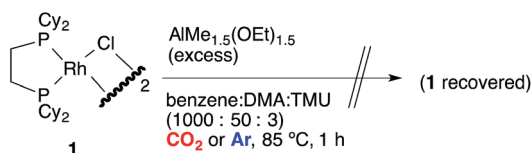
took place successfully under catalytic conditions because the concentration of CO₂ in the liquid phase was much lower than saturation due to its consumption by the carboxylation reaction of RhMe(dcype) **A**. Thus, the dissolution rate of CO₂ controlled the fate of the key intermediate RhMe(dcype) **A**. This clearly indicates that the balance between C–H bond activation and the subsequent transformation is very important for the catalytic C–H bond functionalization reaction using these alkyl metal complexes.

4. Transmetalation behaviors

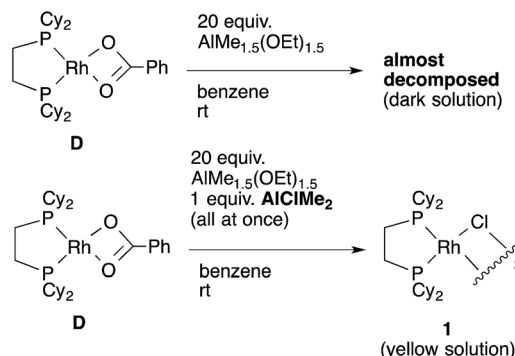
Direct observation of the reaction mixture is a reliable method to obtain information on the resting state of the catalytic cycle. We then observed ³¹P NMR to clarify the rhodium species present in the reaction mixture after the catalytic reaction was carried out in benzene for 1 h under 1 atm CO₂ at 85 °C (Scheme 10). It was a surprise to find that almost no complex except for the starting [RhCl(dcype)]₂ **1** was observed even though benzoic acid was produced gradually. Alternatively, under argon only **1** was observed. No methylrhodium or phenylrhodium species were observed. [RhCl(dcype)]₂ **1** mostly decomposed after 6 h of heating under Ar. Therefore, it was speculated that there would be equilibria between **A–D** and **1**, so that only **1** was observable.

To confirm our speculation, Rh(O₂CPh)(dcype) **D** was prepared and its catalytic activity was examined. When the catalytic carboxylation reaction of benzene was carried out using **D** as a catalyst, benzoic acid was obtained with a TON of only 2.5. In addition, when **D** and excess AlMe_{1.5}(OEt)_{1.5} were mixed in benzene at room temperature (no chloride source), rapid decomposition of the complex was observed using ³¹P NMR (Scheme 11). However, it was found that addition of only an equimolar amount of AlClMe₂ to **D** prevented it from decomposition to give [RhCl(dcype)]₂ **1**, and the catalytic activity was recovered (TON = 28). In other words, the success of the present reaction was due to the fast transmetalation of rather unstable [Rh]–O₂CPh or [Rh]–Me with [Al]–Cl to give a stable dimeric [Rh]–Cl species under catalytic conditions.

The total figure of this reaction is illustrated in Scheme 12. The most important cycle, which provides benzoic acid, is confirmed to be fundamentally the same as we postulated (depicted in bold arrows). First, transmetalation of [RhCl(dcype)]₂ **1** and AlMe_{1.5}(OEt)_{1.5} generates the 14-electron methylrhodium complex, RhMe(dcype) **A**. **A** reacts with benzene to give the 14-electron phenylrhodium complex, RhPh(dcype) **C**, possibly *via* reductive elimination of methane from Rh(H)(Me)(Ph)(dcype) **B**. The following carboxylation of **C** provides rhodium benzoate Rh(O₂CPh)(dcype) **D**. There are two possible pathways in the next step. Transmetalation of **D** and



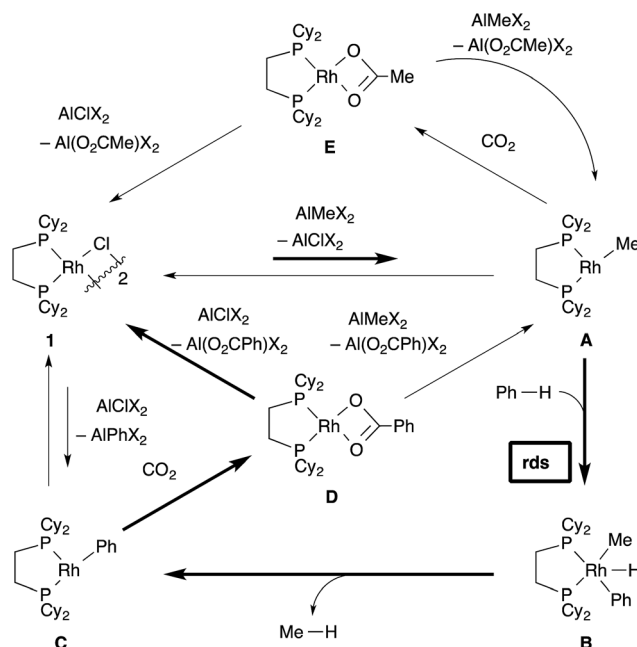
Scheme 10 Analysis of the reaction mixture using ³¹P NMR.



Scheme 11 Transmetalation of Rh–O₂CPh complex.

chloroaluminum species converts the catalyst back to [RhCl(dcype)]₂ **A**, or transmetalation of **D** and methylaluminum species directly gives RhMe(dcype) **A**. However, the generated **A** could be converted to the most thermodynamically stable **1** *via* further transmetalation because of the equilibrium between **1** and **A**.^{24,25} In addition, there is a branch in this reaction. **A** reacts with CO₂ to give Rh(OAc)(dcype) **E** in the same manner as **C**. Therefore, this reaction provides a mixture of acetic acid and benzoic acid.

The undesired formation of **E** should be operative if the reaction mixture contains a sufficient amount of CO₂ in solution. Nevertheless, the desired C–H bond activation takes place because the true concentration of CO₂ in solution is much lower than saturation. Importantly, the catalytic reaction did not work well in the absence of the chloride source. This is probably because the tricoordinated active species, RhMe(dcype) **A** was too unstable to be present at a higher concentration and decomposition of the Rh species occurred. The presence of



Scheme 12 Total figure of the catalytic cycle.



chloride species keeps the resting state of the rhodium species as $[\text{RhCl}(\text{dcype})]_2$ **1**, which has a stable tetracoordinated dimeric structure and moderately reactive to transmetallation with the Al–Me species. This equilibrium limited the concentration of the active species, $\text{RhMe}(\text{dcype})$ **A**, and suppressed its decomposition. Transmetallation steps have attracted less interest in mechanistic studies, and their possible equilibria are mostly ignored. Our observation should be an interesting example to show the importance of the transmetallation equilibria in the catalytic cycle.

Conclusions

This article describes a detailed mechanistic analysis of the rhodium-catalyzed carboxylation of simple aromatic compounds. Although no active intermediates were observable at all in this reaction, the proposed mechanism was mostly supported by several experiments. Most importantly, elucidation of the active species was achieved by designing appropriate precursors, and carrying out kinetic studies. 14-Electron rhodium complexes were found to be the key intermediates in both the C–H bond activation and carboxylation steps. The presence of such species was also supported by the formation of methane and acetic acid. KIE studies under catalytic conditions revealed that the C–H bond activation step was the turnover-limiting step. According to kinetic studies, this C–H bond activation step should be a minor pathway in the presence of a sufficient amount of CO_2 because of undesired predominant carboxylation of the $\text{Rh}^{\text{I}}\text{–Me}$ species. However, further analysis revealed that this problem could be overcome to some extent by mechanical factors such as stirring rate and the shape of the reaction vessel, because undesired carboxylation of the $\text{Rh}^{\text{I}}\text{–Me}$ species could be made slower by controlling the concentration of CO_2 in solution. Finally, it was found that reversible transmetallation pathways to give $[\text{RhCl}(\text{dcype})]_2$ **1** contributed to suppress decomposition of the catalyst. This study will provide new possibilities in such C–H bond functionalization reactions using alkyl-metal species and transition metal-catalyzed carboxylation reactions.

Acknowledgements

This research was supported by JSPS KAKENHI, grant number 24245019, and the ACT-C program from JST. T. S. thanks JSPS for the fellowship.

Notes and references

- 1 Representative reviews on the carboxylation of organic compounds: (a) T. Sakakura, J.-C. Choi and H. Yasuda, *Chem. Rev.*, 2007, **107**, 2365–2387; (b) S. N. Riduan and Y. Zhang, *Dalton Trans.*, 2010, **39**, 3347–3357; (c) M. Cokoja, C. Bruckmeier, B. Rieger, W. A. Herrmann and F. E. Kühn, *Angew. Chem., Int. Ed.*, 2011, **50**, 8510–8537; (d) K. Huang, C.-L. Sun and Z.-J. Shi, *Chem. Soc. Rev.*, 2011, **40**, 2435–2452; (e) Z. Wenzhen and L. Xiaobing, *Chin. J. Catal.*, 2012, **33**, 745–756; (f) Y. Tsuji and T. Fujihara, *Chem.*

- Commun.*, 2012, **48**, 9956–9964; (g) I. Omae, *Coord. Chem. Rev.*, 2012, **256**, 1384–1405; (h) X. Cai and B. Xie, *Synthesis*, 2013, **45**, 3305–3324; (i) J. Takaya and N. Iwasawa, *Science of Synthesis, C-1 Building Blocks in Organic Synthesis*, 2014, vol. 1, pp. 281–307; (j) Q. Liu, L. Wu, R. Jackstell and M. Beller, *Nat. Commun.*, 2015, **6**, 5933.
- 2 T. Suga, H. Mizuno, J. Takaya and N. Iwasawa, *Chem. Commun.*, 2014, **50**, 14360–14363.
- 3 For catalytic C–H bond carboxylation of relatively acidic aromatic compounds, see: (a) I. I. F. Boogaerts and S. P. Nolan, *J. Am. Chem. Soc.*, 2010, **132**, 8858–8859; (b) I. I. F. Boogaerts, G. C. Fortman, M. R. L. Furst, C. S. J. Cazin and S. P. Nolan, *Angew. Chem., Int. Ed.*, 2010, **49**, 8674–8677; (c) L. Zhang, J. Cheng, T. Ohishi and Z. Hou, *Angew. Chem., Int. Ed.*, 2010, **49**, 8670–8673; (d) I. I. F. Boogaerts and S. P. Nolan, *Chem. Commun.*, 2011, **47**, 3021–3024; (e) H. Inomata, K. Ogata, S. Fukuzawa and Z. Hou, *Org. Lett.*, 2012, **14**, 3986–3989.
- 4 $\text{AlMe}_{1.5}(\text{OEt})_{1.5}$ was prepared from AlMe_3 with 2 equiv. of EtOH. The 1 : 1 sharp peaks of the methyl group and ethoxy group indicate this composition and its discrete structure. A tetramer structure has been postulated for the related compound. See: J. Turunen, T. T. Pakkanen and B. Löfgren, *J. Mol. Catal.*, 1997, **123**, 35–42 and ref. 2.
- 5 Examples of stoichiometric C–H bond activation by alkylrhodium(i) complexes: (a) R. T. Price, R. A. Andersen and E. L. Muetterties, *J. Organomet. Chem.*, 1989, **376**, 407–417; The intermediacy of 14-electron alkylrhodium(I) was postulated, however, sufficient experimental supports were not provided. See: (b) S. E. Boyd, L. D. Field, T. W. Hambley and M. G. Partridge, *Organometallics*, 1993, **12**, 1720–1724.
- 6 Stoichiometric carboxylation of arylrhodium(i) complexes: (a) I. S. Kolomnikov, A. O. Gusev, T. S. Belopotapova, M. K. Grigoryan, T. V. Lysyak, Y. T. Struchkov and M. E. Vol'pin, *J. Organomet. Chem.*, 1974, **69**, C10–C12; (b) D. J. Darensbourg, G. Grötsch, P. Wiegrefe and A. L. Rheingold, *Inorg. Chem.*, 1987, **26**, 3827–3830.
- 7 L. Yang and H. Huang, *Chem. Rev.*, 2015, **115**, 3468–3517.
- 8 H. Mizuno, J. Takaya and N. Iwasawa, *J. Am. Chem. Soc.*, 2011, **133**, 1251–1253.
- 9 (a) K. Gao and N. Yoshikai, *Chem. Commun.*, 2012, **48**, 4305–4307; (b) K. Gao, R. Paire and N. Yoshikai, *Adv. Synth. Catal.*, 2014, **356**, 1486–1490.
- 10 B. Zhou, Y. Hu and C. Wang, *Angew. Chem., Int. Ed.*, 2015, **54**, 13659–13663.
- 11 For addition to aldehydes using silanes as stoichiometric reductants, see: (a) Y. Fukumoto, K. Sawada, M. Hagihara, N. Chatani and S. Murai, *Angew. Chem., Int. Ed.*, 2002, **41**, 2779–2781; (b) Y. Kuninobu, Y. Nishina, T. Takeuchi and K. Takai, *Angew. Chem., Int. Ed.*, 2007, **46**, 6518–6520; (c) B.-J. Li and Z.-J. Shi, *Chem. Sci.*, 2011, **2**, 488–493.
- 12 (a) T. G. Ostapowicz, M. Hölscher and W. Leitner, *Chem.–Eur. J.*, 2011, **17**, 10329–10338; (b) H.-L. Qin, J.-B. Han, J.-H. Hao and E. A. B. Kantchev, *Green Chem.*, 2014, **16**, 3224–3229; (c) S. V. C. Vummaleti, G. Talarico, S. P. Nolan, L. Cavallo and A. Poater, *Org. Chem. Front.*, 2016, **3**, 19–23.



